Multiple-Input Multiple-Output Based High Density On-chip Optical Interconnect

Po-Kuan Shen[ab], Xiaochuan Xu[c], Amir Hosseini[c], Zeyu Pan[a], and Ray T. Chen[ac],

[a] Department of Electrical and Computer Engineering, University of Texas at Austin, Austin, Texas 78758, USA
[b] Department of Optics and Photonics, National Central University, Jhong-li,32001, Taiwan
[c] Omega Optics, Inc., Austin, Texas 78757, USA

ABSTRACT

In on-chip optical interconnect, dielectric waveguide arrays are usually designed with pitches of a few wavelengths to avoid crosstalk, which greatly limits the integration density. In this paper, we for the first time propose to use multiple-input multiple-output (MIMO), a well-known technique in wireless communication, to recover the data from entangled signals and reduce the waveguide pitch to subwavelength range. In the proposed on-chip MIMO system, there is significant coupling among the adjacent waveguides in the high density waveguide region. In order to recover signals, the N×N transmission matrix of N high-density waveguides is calculated to describe the relation between each input ports and output ports. In the receiving part, homodyne coherent receivers are used to receive the transmitted signals, and obtain the signal in phase and $\pi/2$ out of phase with local oscillator. In the electrical signal processing, the inverse transmission matrix is utilized to recover the signals in the electronic domain. To verify the proposed on-chip MIMO, we used the INTERCONNECT package in Lumerical software to simulate a 10x10 MIMO system. The cross section of each waveguide is 500 nm x 220 nm. The spacing is 250 nm. The simulation verifies the possibility of recovering 10 Gbps data from the heavily coupled 10 waveguides with a BER better than 10^{-12}. The minimum input optical power for a BER of 10^{-12} is greater than -18.1 dBm, and the maximum phase shift between input laser and local oscillator can reach to 73.5˚.

Keywords: Waveguides, Optical interconnects, Systems

1. INTRODUCTION

Optical interconnect is expected to be widely used for the next generation on-chip interconnects because of providing better propagation delay, energy dissipation, and bandwidth density compared to electrical solution [1, 2]. Based on the viewpoint of bandwidth density, the capacity of optical waveguides is determined by the waveguide geometry and index contrast between waveguide core and cladding [3]. CMOS-compatible silicon waveguide exhibits submicrometer waveguide dimension to support single-mode propagation due to the high index contrast between silicon and its cladding material [4-6]. However, such traditional silicon waveguide array is still designed with pitches of a few wavelengths to avoid significant crosstalk, which greatly limits the integration density for the parallel transmission. Multiple-input multiple-output (MIMO) technique might be one of solutions to improve waveguide bandwidth density. It has been extensively used in wireless communications for a long time [7, 8]. The multiple transmitters and multiple receivers configuration significantly improves system capacity and error probability over traditional single-input single-output systems (SISO) or single-input multiple-output (SIMO) systems. Using the MIMO techniques, several data streams can be transmitted simultaneously over the same multiple parallel paths. Each receiver catches the combination of transmitted data, and then the electrical signal processing techniques is used to decode the transmitted signal. Based on the concept of MIMO techniques, the bandwidth density of on-chip optical interconnect can be improved by using high density waveguide array with subwavelength pitch. If each guiding mode in the high density waveguide region is regarded as a signal path, the high density waveguide array is similar as a wireless channel with tense multipath scattering. Based on the analogy, it is intuitive that MIMO in wireless communication could be applied to high density waveguide arrays. In this letter, we for the first time propose to apply the concept of MIMO system to decouple the entangled signal from a waveguide array with subwavelength pitch. Using MIMO techniques, the waveguide array no

Optical Interconnects XV, edited by Henning Schröder, Ray T. Chen, Proc. of SPIE Vol. 9368, 936812 · © 2015 SPIE · CCC code: 0277-786X/15/$18 · doi: 10.1117/12.2080666

longer need to be kept physically decoupled and the waveguide pitch can be significantly reduced to subwavelength range. Therefore, the bandwidth density can be increased significantly. In this paper, we numerically demonstrated the data transmission of 10-Gbps through 10 heavily coupled waveguides with 250 nm spacing.

2. DESIGN OF ON-CHIP MIMO SYSTEM

Figure 1 shows the block diagram of N×N on-chip MIMO system. It consists of transmitters, N high density waveguides, homodyne coherent receivers, and electrical signal processing components. In the transmitters, each input laser, which possesses same wavelength, phase, and optical power, is launched into the individual optical amplitude modulator and then fed into the high density silicon waveguide array. In the N high density waveguides, there is significant coupling among the adjacent waveguides due to the subwavelength waveguide pitch. As a result, a number of signal streams are transmitted simultaneously over the same multipath channels and randomly combined in each receiver. In order to recover these entangled signals, the N×N transfer matrix is needed to define the relation between j-th input port and i-th output port, as shown in following:

$$\begin{bmatrix} O_1 \\ \vdots \\ O_i \\ \vdots \\ O_N \end{bmatrix} = \begin{bmatrix} T_{11} & \cdots & T_{1j} & \cdots & T_{1N} \\ \vdots & & \vdots & & \vdots \\ T_{i1} & \vdots & T_{ij} & \vdots & T_{iN} \\ \vdots & & \vdots & & \vdots \\ T_{N1} & \cdots & T_{Nj} & \cdots & T_{NN} \end{bmatrix} \begin{bmatrix} I_1 \\ \vdots \\ I_j \\ \vdots \\ I_N \end{bmatrix} \quad (1)$$

where $[T_{ij}]$ is the transfer matrix of high density waveguides, $[I_j]$ is the input signal, and $[O_i]$ is the output signal. All matrix elements are complex numbers as they take into account both amplitude and phase of electric field at each input and output port of high density silicon waveguide array.

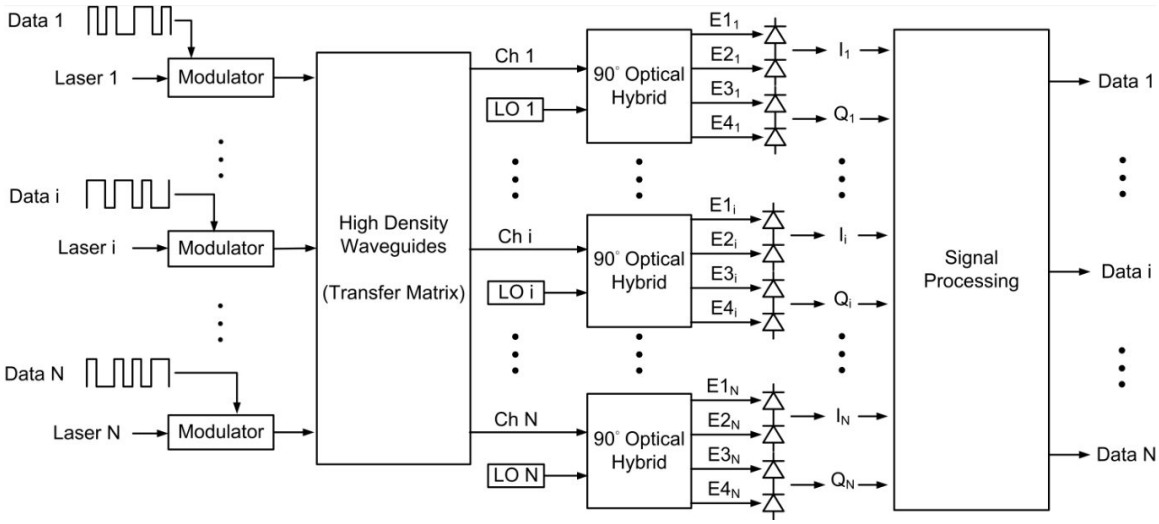

Fig. 1. The block diagram of proposed N×N on-chip MIMO system operating over the high density silicon waveguide array

Then the homodyne coherent receiver is used to detect the transmitted signals. In the homodyne coherent receiver, the local oscillator which has the same frequency, phase, and amplitude as input laser is the key to lock the phase of the incoming optical signals [9]. The superposed electrical field ($\sum_{j=1}^{N} E_{ij}$) from each input channels and local oscillator (E_{Li}) are directed into the quadrature optical hybrid which gives four outputs:

$$E1_i = \frac{1}{2}\left(\sum_{j=1}^{N} E_{ij} + E_{Li}\right) \quad (2)$$

$$E2_i = \frac{1}{2}\left(\sum_{j=1}^{N} E_{ij} - E_{Li}\right) \quad (3)$$

$$E3_i = \frac{1}{2}\left(\sum_{j=1}^{N} E_{ij} + jE_{Li}\right) \quad (4)$$

$$E4_i = \frac{1}{2}\left(\sum_{j=1}^{N} E_{ij} - jE_{Li}\right) \quad (5)$$

By applying (2) and (3), and (4) and (5) to two PIN photodetectors (PDs), it provides the I_i and Q_i components which is given by

$$I_i = I_{E1i} - I_{E2i} = R\sum_{j=1}^{N}\sqrt{P_{ij}P_{Li}}\cos(\theta_{ij} - \theta_{Li}) \quad (6)$$

$$Q_i = I_{E3i} - I_{E4i} = R\sum_{j=1}^{N}\sqrt{P_{ij}P_{Li}}\sin(\theta_{ij} - \theta_{Li}) \quad (7)$$

where R is the responsivity of PD, P_{ij} is the optical power from j-th input port to i-th output port, P_{Li} is the optical power of local oscillator at i-th receiver, θ_{ij} is the phase of received signal from j-th input port to i-th output port, and the θ_{Li} is phase of local oscillator at i-th receiver. I_i and Q_i represent the photodetector current from optical signals in phase and $\pi/2$ out of phase with local oscillator, respectively. These are applied to recover the transmitted signal in signal processing. Figure 2 shows the schematic signal processing, it consists of two steps: 1) calculating the real parts (G_R) and image parts (G_I) of inverse transfer matrix and 2) using the inverse transfer matrix to calculate the recovered data by two adders and subtractors. Each I_i and Q_i from the homodyne coherent receivers are fed into the real parts and image parts of inverse transmission matrix, and two adders and subtractors are employed to calculated the real parts (R_i) and image parts (M_i) of recovered data, it enable the signal to transmit from multiple input ports and receive by multiple output ports. The calculated formulas are shown in below:

$$R_i = I_i \times G_R - Q_i \times G_I \quad (8)$$

$$M_i = Q_i \times G_R + I_i \times G_I \quad (9)$$

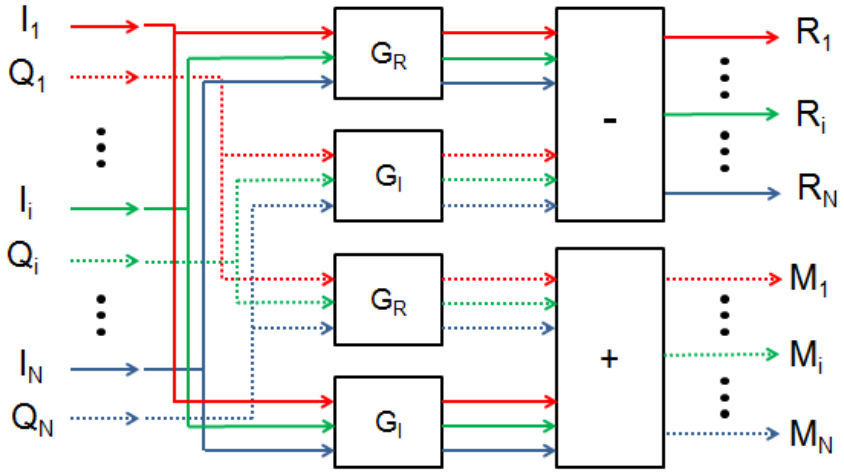

Fig. 2. The schematic signal processing for the N×N on-chip MIMO system

3. 10×10 ON-CHIP MIMO SYSTEM

Based on the above discussion, we simulated the performance of a 10×10 on-chip MIMO system comprised of a high density waveguide array of ten silicon strip waveguides, coherent detection, and signal processing. In this letter, the MODE Solution package in Lumerical software is used to simulate the 10 high density waveguides and calculate the transfer matrix of high density parallel silicon waveguides. Figure 3(a) schematically shows the cross-section of 10 high density parallel silicon waveguides. The cross section (W×H) of each waveguide is 500×220 nm with refractive indices of 3.4764. The spacing (S) is 250 nm. The waveguide length is 1 mm. The thickness of SiO_2 buried oxide (BOX) layer is 2 μm and the refractive index is 1.444 [10]. Figure 3(b) shows the simulated electric field magnitude distribution of the 10 high density waveguides at 1550 nm. The mode coupling between adjacent waveguides is strong due to the extremely tight waveguide spacing of 250 nm. To decode the transmitted signals, the matrix is obtain by sequentially exciting each waveguide with the fundamental TE mode and records the amplitude and phase of electric field at each output port. This makes it possible to determine the transfer matrix and further calculate the inverse transfer matrix for the signal processing.

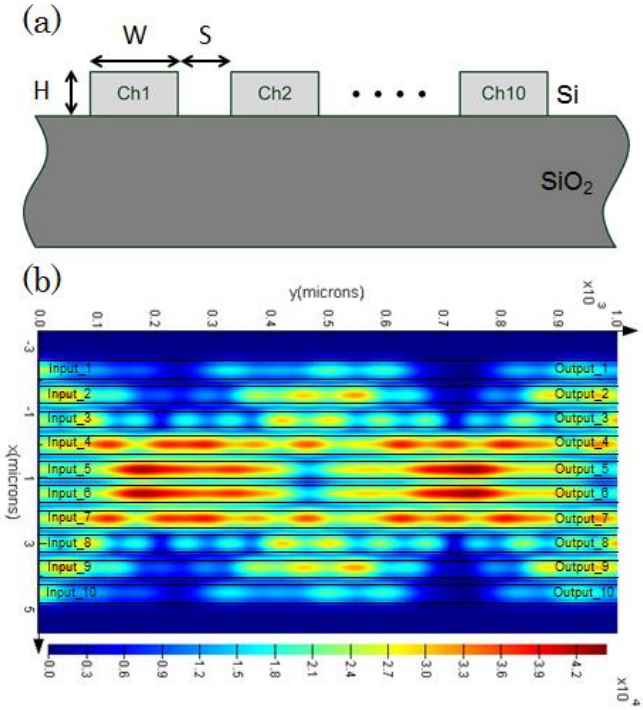

Fig. 3. (a) The schematic cross-section of 10 high density parallel silicon waveguides with 250 nm spacing. (b) The electric field magnitude distribution in the 10 high density parallel silicon waveguides.

To verify the 10×10 on-chip MIMO system, we used the INTERCONNECT package in Lumerical software to simulate the whole system, including waveform recovery, eye diagram, input optical power requirement, and phase shift between input laser and local oscillator. In the simulation model, the high density waveguides are replaced by the 10×10 transfer matrix. In the transmitter part, 10 lasers with wavelength of 1550 nm, relative intensity noise (RIN) of -145 dB/Hz, and optical power of 0 dBm are fed into optical amplitude modulators which are modulated by 10-Gbps non-return-to-zero (NRZ) high-speed electrical signals with a pseudo-random bit sequence (PRBS) of 2^{31}-1 and quality factor of 16. All of these values refer to the Agilent N4872A ParBERT modules and the commercial distributed feedback (DFB) lasers. In the receiver part, the local oscillators possess the same characteristic as input laser. The PDs with responsivity of 0.8 W/A, dark current of 10 nA, and thermal noise of 10^{-22} are utilized to detect the transmitted optical signals. The 3-dB frequency bandwidth of PDs is 22 GHz (Discovery Semiconductors DSC30S).

Figure 4 shows the recovered eye diagram and waveform comparison between input electrical signals and output recovered signals. Figure 4(a) shows the input electrical signal waveform in the channel 5. The amplitude of input electrical signal is 0.6 a.u.. The noise caused by the internal electrical noise source and random jitter of 1.5 ps is used to define the quality factor of input electrical signals. Figure 4(b) shows the recovered signal waveform. The simulation proves that it is possible to recover signals from 10 heavily coupled waveguides with 250 nm spacing. Compared with the input signals, the amplitude of recovered waveform approximately reduce to 0.35 a.u., it's due to the PDs responsivity of 0.8 A/W and the electrical signal process. Figure 4(c) shows the recovered eye diagram at 10 Gbps. The simulated quality factor is 15.54, and the peak-to-peak jitter is 10.69 ps. The clear eye diagrams demonstrate that the proposed on-chip MIMO system possess the facility in data transmission at 10 Gbps with high density waveguides.

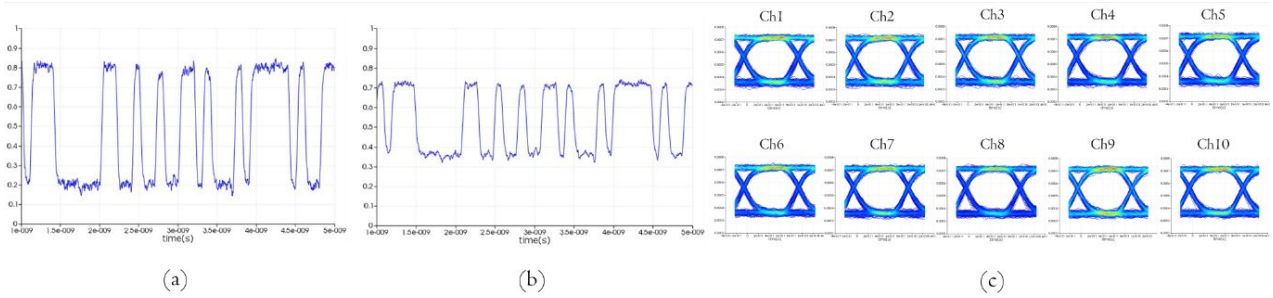

Fig. 4. (a) The input electrical signal waveform in the channel 5. The electrical noise source and random jitter of 1.5 ps is used to define the quality factor of input electrical signals. (b) The recovered signal waveform in the channel 5. (c) The recovered eye diagram for 10×10 on-chip MIMO system

In order to evaluate the system performance, we simulate the bit error rate (BER) as a function of the input optical power for the 3×3, 5×5, and 10×10 on-chip MIMO system. In each channel, the input power is controlled by a variable optical attenuator (VOA) before entering the high density waveguide array. The optical power requirement can be characterized through adjusting the VOAs and monitoring the BER at the receivers. Figure 5(a) to (c) show the simulation result of the proposed 3×3, 5×5, and 10×10 on-chip MIMO system, respectively. For these cases, the input optical power is attenuated from -17 to -23 dBm. The BER is smaller than 10^{-12} when the input optical power is larger than -18.72, -18.37, and -18.18 dBm in the case of 3×3, 5×5, and 10×10, respectively. Figure 5(d) shows the Box chart of input optical power at the BER of 10^{-12} for each MIMO system. There is no obviously decrease in minimum input optical power when the number of waveguides increases. The error-free data transmission could be achieved. However, the variation range of input optical power between each channel increases when the amount of waveguide increases. The optical power variation at BER of 10^{-12} is observed as 1.27, 4.2, and 5.02 μW for the case of 3×3, 5×5, and 10×10, respectively. It is probably due to the disturbance of individual noise in each input electrical signals.

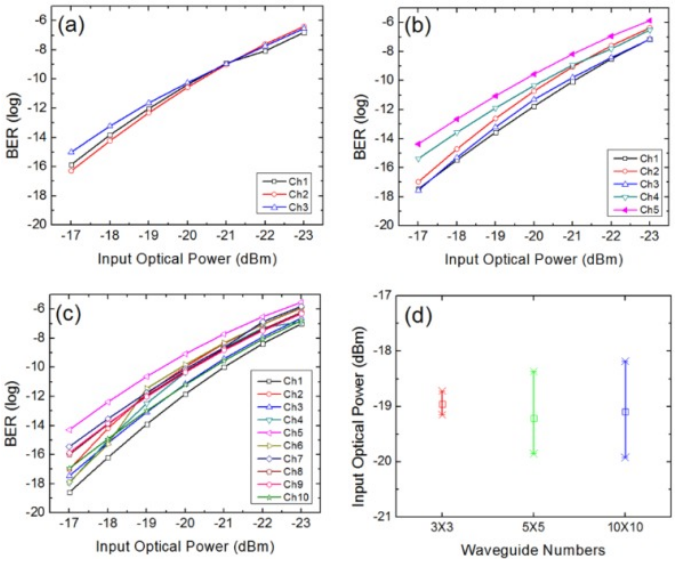

Fig. 5. The simulated BER as a function of the input optical power for the (a) 3×3, (b) 5×5, and (c) 10×10 on-chip MIMO systems. The BER could be smaller than 10^{-12} when the received optical power is larger than -18.1 dBm.

Since the coherent detection is utilized in the receiver, the phase variation caused by the high density waveguides and quadrature optical hybrid is a key issue for the signal recovery. In order to verify the performance of coherent detection for the 10×10 on-chip MIMO system, we synchronously adjust the phase of all local oscillators to produce the phase shift between input laser and local oscillator. Figure 6 shows the BER as the function of phase shift between input laser and local oscillator. The simulation proves that the maximum phase shift is 73.5˚, which is defined to achieve the fixed BER of 10^{-12}. The irregular behave in the ch2 and ch7 at phase shift is due to the randomly electrical noise from the input electrical signal.

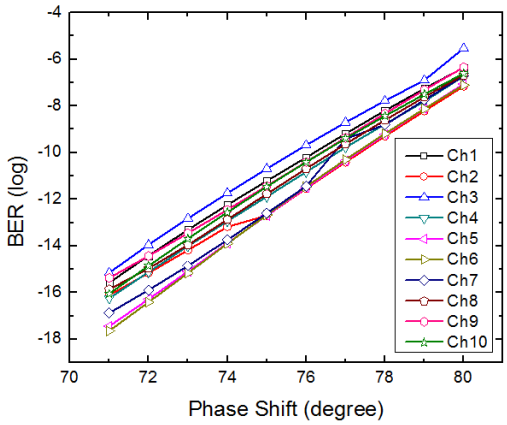

Fig. 6. The simulated BER as a function of the phase shift between input laser and local oscillator. The maximum phase shift is 73.5˚ when BER is greater than 10^{-12}.

4. CONCLUSION

We for the first time propose to apply the MIMO in wireless communication to high density on-chip optical interconnect. Usually, the spacing between two adjacent waveguides needs to be a few wavelengths to avoid crosstalk. With MIMO, it is possible to recover data from entangled signals and therefore reduce the waveguide spacing to subwavelength range. The simulation proves that it is possible to recover 10 Gbps data from 10 heavily coupled waveguides with 250 nm spacing. The BER is better than 10^{-12}, and the minimum input optical power for a BER of 10^{-12} is greater than -18.1 dBm.

REFERENCES

[1] D. A. B. Miller, "Device requirements for optical interconnects to silicon chips," Proceedings of the IEEE, vol. 97,no. 7 pp. 1166-1185, July 2009

[2] Raymond G. Beausoleil, Philip J. Kuekes, Gregory S. Snider, Shih-Yuan Wang, and R. Stanley Williams, "Nanoelectronic and nanophotonic interconnect," Proceedings of the IEEE, vol. 96, no. 2, pp. 230-247, Feb. 2008

[3] Mikhail Haurylau, Guoqing Chen, Hui Chen, Jidong Zhang, Nicholas A. Nelson, David H. Albonesi, Eby G. Friedman, and Philippe M. Fauchet, "On-chip optical interconnect roadmap: challenges and critical directions," IEEE J. Sel. Top. Quant. Electron., vol. 12, no. 6, pp. 1699-1705, Dec. 2006

[4] Guoliang Li, Jin Yao, Ying Luo, Hiren Thacker, Attila Mekis, Xuezhe Zheng, Ivan Shubin, Jin-Hyoung Lee, Kannan Raj, John E. Cunningham, and Ashok V. Krishnamoorthy, "Ultralow-loss, high-density SOI optical waveguide routing for macrochip interconnects," Opt. Express, vol. 20, no. 11, pp. 12035-12039, May 2012

[5] Po Dong, Wei Qian, Shirong Liao, Hong Liang, Cheng-Chih Kung, Ning-Ning Feng, Roshanak Shafiiha, Joan Fong, Dazeng Feng, Ashok V. Krishnamoorthy, and Mehdi Asghari, "Low loss shallow-ridge silicon waveguides," Opt. Express, vol. 18, no. 14, pp. 14474-14479, Jun. 2010

[6] Yangyang Liu, Jeffrey M. Shainline, Xiaoge Zeng, and Miloš A. Popović, "Ultra-low-loss CMOS-compatible waveguide crossing arrays based on multimode Bloch waves and imaginary coupling," Optics Letters, vol. 39, no. 2, pp. 335- 338, Jan. 2014

[7] Michael A. Jensen and Jon W. Wallace, "A review of antennas and propagation for MIMO wireless communications," IEEE Trans. Antennas Propag., vol. 52, no. 11, pp. 2810-2824, Nov. 2004

[8] David Gesbert, Mansoor Shafi, Da-shan Shiu, Peter J. Smith, and Ayman Naguib, "From theory to practice: an overview of MIMO space–time coded wireless systems," IEEE J. Sel. Areas Com., vol. 21, no. 3, pp. 281-302, Apr. 2003

[9] Ezra Ip, Alan Pak Tao Lau, Daniel J. F. Barros, Joseph M. Kahn, "Coherent detection in optical fiber systems," Opt. Express, vol. 16, no. 2, pp. 753-791, Jan. 2008

[10] I. H. MALITSON, "Interspecimen comparison of the refractive index of fused silica," J. Opt. Soc. Am., vol. 55, no. 10, pp. 1205-1209, Oct. 1965